

See discussions, stats, and author profiles for this publication at: <https://www.researchgate.net/publication/244446643>

# Water and Polymer Mobility in Hydrogel Biomaterials Quantified by $^1\text{H}$ NMR: A Simple Model Describing Both $T_1$ and $T_2$ Relaxation

ARTICLE *in* MACROMOLECULES · AUGUST 2002

Impact Factor: 5.8 · DOI: 10.1021/ma020539c

---

CITATIONS

30

---

READS

22

3 AUTHORS, INCLUDING:



**Patrick Mcconville**

Molecular Imaging Inc

50 PUBLICATIONS 1,088 CITATIONS

SEE PROFILE



**James M Pope**

Queensland University of Technology

127 PUBLICATIONS 3,087 CITATIONS

SEE PROFILE

# Water and Polymer Mobility in Hydrogel Biomaterials Quantified by $^1\text{H}$ NMR: A Simple Model Describing Both $T_1$ and $T_2$ Relaxation

Patrick McConville, Michael K. Whittaker, and James M. Pope\*

Centre for Medical, Health and Environmental Physics, School of Physical and Chemical Sciences, Queensland University of Technology, Brisbane, Australia 4001

Received April 4, 2002

**ABSTRACT:**  $^1\text{H}$  NMR  $T_1$  relaxation has been measured in a series of commercially available contact lens hydrogels of varying composition and equilibrium water content (EWC). Using previously published  $T_2$  relaxation data for the same materials, the data were analyzed using a relatively simple model incorporating magnetization transfer between water and polymer protons. It was found that both data sets were generally well described using common fit parameters. Analysis of the fitted parameters suggests that the average water mobility in these materials is largely governed by the EWC, although at a given EWC, slightly increased mobility (decreased average binding) was found in the IGEL materials that possess no exchangeable protons on the polymer chains. The combination of  $T_1$  and  $T_2$  measurements in a single model allows more accurate quantification of water and polymer mobility and binding in these hydrogels. The methodology outlined in this study should also be applicable to other hydrogel systems.

## Introduction

Hydrogels, polymers that swell in water to form soft elastic gels, have found widespread use in biomedical applications ranging from implant materials to soft contact lenses.<sup>1</sup> Underpinning the successful use of hydrogels in these applications has been their water absorption and permeation properties. With the increasing use of hydrogels in applications where the diffusive transport of the water molecules is important, such as drug delivery platforms, tissue scaffolding, and membranes in filtration devices, it is of great importance to understand how the polymer network changes the behavior of the imbued water. The motivation of the present study was to attempt to quantify the binding and mobility of the water molecules in hydrogel materials used for soft contact lens manufacture. It is anticipated that this may lead to a better understanding of the tendency of these contact lenses to dehydrate when placed on the eye.

The mobility of water in a hydrogel is modified relative to the bulk form due to the presence of boundaries and interfaces arising from the network structure of the polymer, which physically constrain the mobility of water molecules through electrostatic interaction and hydrogen bonding. Water molecules may be preferentially located or partitioned at hydrophilic sites with high enthalpies of adsorption and high barriers to translation. These two effects are synergistic in nature and may be expected to introduce a degree of anisotropy in the molecular motion as well as affecting its time scale. However, despite the many techniques used to investigate the behavior of water in hydrogel materials, including dielectric spectroscopy,<sup>2</sup> gravimetric desorption,<sup>3</sup> X-ray and neutron scattering,<sup>2</sup> differential scanning calorimetry,<sup>4</sup> and nuclear magnetic resonance (NMR) techniques,<sup>5–7</sup> a detailed picture of the state of water in hydrogels remains unclear.

Proton NMR has the potential to quantify water binding and mobility and has been applied to the study

of hydrogel contact lenses, through measurements of the spin–spin ( $T_2$ ) and spin–lattice ( $T_1$ ) relaxation times<sup>8–10</sup> as well as the self-diffusion coefficient.<sup>11</sup> However, it has been shown that hydrogels exhibit complex NMR relaxation behavior due to the effects of magnetization transfer between water and polymer protons which may occur through chemical exchange and/or cross-relaxation. Further complexity can arise through the existence of multiple correlation times for each exchanging species.

In recent published work, McConville and Pope<sup>9</sup> have demonstrated that valuable information about the mobility of water in commercially available contact lenses can be extracted from  $T_2$  NMR relaxation data using a relatively simple model, provided that the influence of chemical exchange on the measured  $T_2$  values is considered. It was shown that the motion of the water in these hydrogels could be adequately characterized by invoking just two correlation times. However, while analysis of the  $T_2$  data provided insight into the longer correlation time component, it proved insensitive to the shorter correlation time motion.

To investigate the faster component of motion of the water molecules, we have applied the same two-site exchange model (developed for modeling of  $T_2$  relaxation data) to the analysis of the variation in  $T_1$  relaxation times with temperature for some of these same materials. The aim of this work was to determine whether this relatively simple model could describe both  $T_1$  and  $T_2$  data with a common set of motional correlation times and thereby provide a consistent picture of the state and mobility of water in a wide range of hydrogel biomaterials. Since  $T_1$  and  $T_2$  relaxation are sensitive to molecular motions on very different time scales, it was proposed that a single model incorporating fits to both  $T_1$  and  $T_2$  data would provide a more accurate description of the complex molecular motions occurring on widely varying time scales in the hydrogel. This would add validity to the model as well as help to refine the fitted parameters that describe the motional behavior of the water and the polymer.

\* To whom correspondence should be addressed. Fax +61-7-3864-1521; e-mail j.pope@qut.edu.au.

**Table 1. Composition<sup>18,19</sup> and Measured EWC of the Hydrogels Used in the Study<sup>a</sup>**

hydrogel name	polymer composition	measured EWC at 80 °C (% w/w)
IGEL 58	NVP/MMA	37.8
IGEL 67	NVP/MMA	49.7
IGEL 77	NVP/MMA	63.7
Benz 38	HEMA	34.7
Benz G-3x	HEMA/GMA	43.9
Benz G-5x	HEMA/GMA	56.1
Benz G-7x	HEMA/GMA	74.5

<sup>a</sup> EWC was measured as % w/w relative to the total mass of the hydrated material. NVP = *N*-vinylpyrrolidone, MMA = methyl methacrylate, HEMA = hydroxyethyl methacrylate, GMA = glycerol methacrylate.

## Experimental Section

**Sample Protocol.** A set of commercially available contact lens hydrogels in the Benz and IGEL ranges were supplied by Benz Research and Development Corp., Sarasota, FL, and Capricornia Contact Lens, Brisbane, Australia, respectively. The commercial names of these materials, together with their composition and EWCs (measured at 80 °C), are shown in Table 1. All materials were supplied in the dry state. To produce hydrogels, the dry material was allowed to equilibrate in phosphate buffered saline (PBS) in sealed vials at 80 °C for at least 1 week. PBS is a standard diluent used to hydrate commercial contact lenses and has constituents that mimic the pH and osmolality of the tears. The equilibration temperature was chosen because this was the highest temperature at which NMR measurements were to be made. Hydrogels, being elastomers, contract on heating with a consequent reduction in EWC. By equilibrating at this temperature, loss of water from the gel during the NMR experiments was minimized. Where appropriate, a duplicate series of materials were also prepared in PBS solution that had been made up using deuterated water (PBS/D<sub>2</sub>O). This effectively removed the signal due to the water protons in the NMR experiments, allowing the contribution of nonexchangeable protons on the polymer to be determined.

Prior to each experiment, samples were blotted thoroughly and quickly with lint free tissue, wrapped in clear polyethylene ("clingwrap") film, and placed in an NMR tube. The film helped prevent excessive dehydration during the measurements. A Teflon vortex plug was also inserted just above the sample to limit air convection in the NMR tube and ensure moisture loss from the gel was kept to a minimum. Following the NMR measurements, the sample was removed and reweighed and the water loss (if any) calculated. In all cases this water loss was less than 5%.

**NMR Measurements.** Experiments were carried out using a Bruker MSL200 NMR spectrometer operating at 200 MHz for protons. A variable temperature control unit allowed the temperature of the sample to be maintained to an accuracy of  $\pm 1$  °C. The sample was allowed to equilibrate at each temperature for 15 min, after which the spectrometer operating parameters (e.g., <sup>1</sup>H pulse lengths, shim settings, etc.) were optimized. Prior to the *T*<sub>1</sub> measurement, a free induction decay (FID) signal was acquired, the <sup>1</sup>H spectrum examined, and the line width of the <sup>1</sup>H peak measured.

*T*<sub>1</sub> measurements were performed using a standard inversion recovery pulse sequence at temperatures ranging from 80 °C down to -30 °C in 10 °C intervals. This allowed a relatively wide range of temperatures centered approximately about room temperature and physiological temperature (the most relevant temperatures applying to hydrogel biomaterials) to be examined. To confirm that temperature equilibrium had been achieved and to check for reproducibility, a repeat *T*<sub>1</sub> measurement was made 15 min after the original measurement for selected samples. A total of 16 data points were collected during each inversion recovery experiment with the maximum pulse spacing adjusted to ensure a plateau in the recovery of longitudinal magnetization had been achieved. The

*T*<sub>1</sub> relaxation times were determined by using a Levenberg–Marquardt nonlinear least-squares fitting routine to fit the data to a single-exponential rise to a maximum asymptotic value, using two free parameters (*T*<sub>1</sub> and *I*<sub>0</sub>, the signal intensity at zero time).

## Theory

**The Exchange Model for *T*<sub>2</sub> Relaxation.** In heterogeneous polymer systems, the observed <sup>1</sup>H NMR relaxation (*T*<sub>1</sub> and *T*<sub>2</sub>) behavior is determined both by the intrinsic relaxation behavior of each of the (motionally inequivalent) proton populations or "pools" and by the effects of magnetization transfer that may occur between them. We have shown previously<sup>9</sup> that the variation of the spin–spin relaxation time, *T*<sub>2</sub>, with temperature for hydrogel systems in the presence and absence of chemical exchange of protons between water and polymer (depending on the copolymer composition; see below) is well described by the following equation:

$$\frac{1}{T_{2(\text{measured})}} = \frac{1 - p_c}{T_{2b}} + \frac{p_c}{T_{2c} + \tau_{\text{ex}}} \quad (1)$$

where *T*<sub>2(measured)</sub> is the observed *T*<sub>2</sub> of the polymer/water system, and *p*<sub>c</sub> is the ratio of the number of exchangeable protons to the total proton pool, comprising water protons, labeled the "b" species, and exchangeable polymer protons, labeled the "c" species. *T*<sub>2b</sub> and *T*<sub>2c</sub> are the intrinsic transverse relaxation times of these two proton populations, and  $\tau_{\text{ex}}$  is the exchange correlation time (the rate constant for the exchange process being  $1/\tau_{\text{ex}}$ ). The parameter *p*<sub>c</sub> is a constant for a particular material that can be readily determined on the basis of the composition and EWC of the hydrogel in question. Equation 1 has previously also been applied to transverse relaxation in polysaccharide-based gels.<sup>12,13</sup> However, it is strictly valid only in the limit *p*<sub>c</sub>  $\ll$  1, which is a reasonable approximation for relatively high EWC materials.

In the Benz materials, the b and c proton populations are coupled through chemical exchange, with the exchangeable polymer protons originating from hydroxyl (OH) protons on the HEMA side chains. In the IGEL materials, no such exchange mechanism exists, so that in this case *p*<sub>c</sub> = 0.

**Anisotropic Molecular Motion.** "Bound" or motionally restricted molecules may be expected to exhibit motion on more than one distinguishable time scale. Depending on the time scale of these motions, they may separately influence the dipolar interactions, leading to complex NMR relaxation behavior. In general, a distribution of correlation times is likely to be more realistic representation of anisotropic motion; however, use of as few as two dominant correlation times can be shown to be a good approximation in many cases.

In our previous work, it was found that the water proton relaxation could be described in terms of a population-weighted average of two relaxation rates, characterized by motional correlation times labeled "bf" (for the faster motion) and "bs" (for the slower motion), such that

$$\frac{1}{T_{2b}} = \frac{w_{\text{bf}}}{T_{2\text{bf}}} + \frac{w_{\text{bs}}}{T_{2\text{bs}}} \quad (2)$$

However, it should be noted that we cannot distinguish between the case where more than one species of water

molecules each exhibits distinguishable motional behavior and the separate case in which a *single* species of water molecules exhibits anisotropic reorientation.

**The Exchange Model for  $T_1$  Relaxation.** It might be anticipated that a similar expression to that of eq 1 could also be used to describe  $T_1$  relaxation behavior in these systems. However, in the  $T_1$  experiment the population of polymer protons contributing to the measured relaxation in general is *not* restricted to exchangeable polymer protons. Between the 180° and 90° pulses in a conventional inversion recovery sequence used to measure  $T_1$ , longitudinal magnetization is rapidly dispersed across all the protons in the polymer by efficient spin diffusion (the so-called “spin flip-flop” process). Therefore, in materials that contain exchangeable polymer protons (the Benz series), coupling of water and polymer proton magnetization through chemical exchange means that all polymer protons will contribute to the measured  $T_1$  relaxation.

As a result, in the case of  $T_1$  the weighting term,  $p_c$ , used in the  $T_2$  expression must be replaced by a parameter  $P_c$  equal to the relative proportion of polymer protons to the total number of polymer and water protons. This new weighting factor does not satisfy the condition of  $P_c \ll 1$ , even for hydrogels of high EWC. Consequently, a more general equation<sup>14</sup> is required to describe the longitudinal relaxation:

$$\frac{1}{T_{1(\text{measured})}} = \frac{1 - P_c}{T_{1b}} \left[ \frac{\tau_{\text{ex}} + T_{1c}}{(1 - P_c)\tau_{\text{ex}} + T_{1c}} \right] + \frac{P_c}{T_{1c} + \tau_{\text{ex}}(1 - P_c)} \quad (3)$$

Here  $T_{1(\text{measured})}$  is the observed  $T_1$  of the polymer/water system and  $T_{1b}$  the intrinsic relaxation time of the water proton pool, with  $P_c$  and  $T_{1c}$  the relative proportion and intrinsic relaxation time, respectively, of those polymer protons that contribute to longitudinal relaxation. Again,  $P_c$  is a constant that can be determined from the hydrogel composition and EWC.

Information about the molecular motions can be extracted from variable temperature data for  $T_1$  by first invoking a simple Bloembergen Purcell and Pound (BPP) description for the intrinsic  $T_1$  relaxation rate corresponding to each pool. The BPP theory assumes rapid molecular motional averaging, a reasonable assumption in the materials we used which were fully hydrated and not subjected to temperatures where significant freezing of the water occurred. The following equation describes the dependence of  $T_1$  on the correlation time ( $\tau_c$ ) for the motion of molecules in a particular pool:

$$\frac{1}{T_1} = C \left[ \frac{\tau_c}{1 + \omega_0^2 \tau_c^2} + \frac{4\tau_c}{1 + 4\omega_0^2 \tau_c^2} \right] \quad (4)$$

Here  $\omega_0$  is the resonant frequency and the constant  $C$  is a measure of the strength of the magnetic dipolar interactions that couple the protons. In this work a value for  $C$  derived for geminal water protons ( $5.33 \times 10^9 \text{ s}^{-20}$ ) has been assumed.<sup>15</sup> An Arrhenius activation law can then be used to describe thermal activation of the molecular motion:

$$\tau_c = \tau_0 e^{E_A/kT} \quad (5)$$

where  $\tau_0$  is the “Arrhenius coefficient” and  $E_A$  is the activation energy of the motional process under consideration. In the limits  $\omega_0\tau \ll 1$  and  $\omega_0\tau \gg 1$  an “Arrhenius plot”, or a plot of  $\ln(T_1)$  or  $\ln(T_2)$  vs  $T^{-1}$ , describes a straight line with slope  $\pm E_A$ .

**The  $T_1$  Model for Polymers with No Exchangeable Protons.** For materials that contain no exchangeable polymer protons (e.g., IGEL), only “through-space” cross-relaxation between the polymer and water proton populations can contribute to water–polymer proton magnetization transfer in these materials. However, this process is most efficient in rigid networks where neighboring protons are highly coupled and have characteristic short  $T_2$ . The process will be relatively inefficient between the polymer and water, since the approach of a water proton to a polymer proton is limited by the length of hydrogen bonds, and the tendency for water protons to diffuse and exchange rapidly among each other limits the strength of the coupling. Therefore, as a first approximation in materials with no exchanging polymer protons, this contribution can be assumed to be negligible ( $P_c = 0$  and  $\tau_{\text{ex}} = \infty$ ), so that  $T_{1(\text{measured})} = T_{1b}$ . If the water molecules exhibit anisotropic or multiple correlation time behavior, similar to the  $T_2$  case (see eq 2), as a first approximation of this behavior, we can write

$$\frac{1}{T_{1(\text{measured})}} = \frac{1}{T_{1b}} = \frac{w_{\text{bf}}}{T_{1bf}} + \frac{w_{\text{bs}}}{T_{1bs}} \quad (6)$$

where  $T_{1bf}$  and  $T_{1bs}$  are the intrinsic  $T_1$ 's of the short correlation time (fast molecular motion) and long correlation time (slow motion) components describing the water proton relaxation, respectively, and  $w_{\text{bf}}$  and  $w_{\text{bs}}$  ( $w_{\text{bf}} + w_{\text{bs}} = 1$ ) are their corresponding weighting factors.

## Results

Careful analysis of the relaxation data revealed that, for the hydrogel materials described in this study, both  $T_1$  and  $T_2$  relaxation were well represented by single-exponential recovery curves. That is, the signal from (nonexchangeable) polymer protons was not observed as a second component. This is because for  $T_2$  measurements, the interpulse spacing (2.4 ms) was not short enough to refocus magnetization from these protons, and for  $T_1$  measurements, the signal from any short  $T_2$  components (polymer protons) would have decayed substantially during the 100  $\mu\text{s}$  delay between the readout 90° pulse and the commencement of signal acquisition. Because of this delay, unless there is efficient magnetization transfer between the polymer and water protons in the hydrogels, the signal from the polymer protons is effectively dephased and does not make a measurable contribution to the observed  $T_1$ . Where there is sufficiently rapid coupling between the water protons and those of the polymer, as in the case of the Benz materials (see below), this coupling ensures that all the protons in the sample decay with a single longitudinal relaxation time.

**$T_1$  and  $T_2$  Temperature Dependency and Fitting—IGEL Data.** Figures 1 and 2 are Arrhenius plots of the temperature dependence of  $T_1$  and  $T_2$  for the IGEL 58, 67, and 77 hydrogels equilibrated at 80 °C in PBS. The (nonlinear) behavior of the  $T_1$  data suggests that, as in the case of the  $T_2$  data reported previously,<sup>9</sup> the



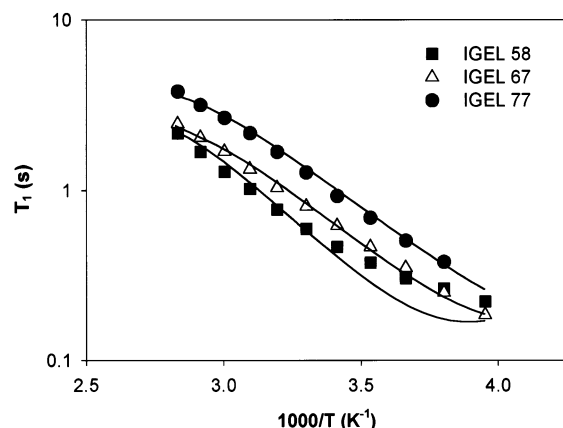


**Figure 1.**  $\ln(T_1)$  as a function of  $1/T$  for the IGEL materials. The solid lines are fits to eq 1 with  $p_c = 0$ , using parameters common to the  $T_2$  fits shown in Figure 2.

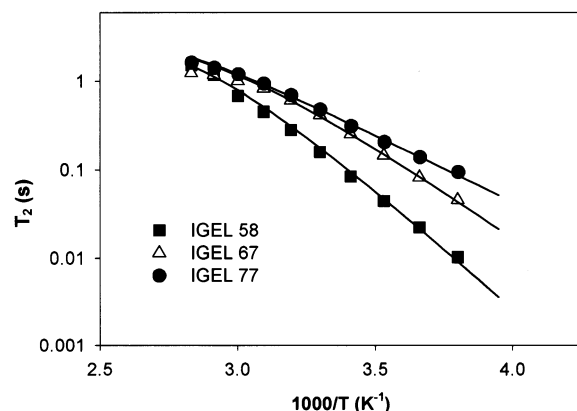


**Figure 2.**  $\ln(T_2)$  as a function of  $1/T$  for the IGEL materials. The solid lines are fits to eq 6, using parameters common to the  $T_1$  fits shown in Figure 1.

relaxation behavior must be described by more than one correlation time.

The IGEL materials are a copolymer series of *N*-vinylpyrrolidine and methyl methacrylate, neither of which contains exchangeable protons. Therefore, eq 6 was initially used to fit the data. As in the case of the corresponding  $T_2$  data, the multiple correlation times must then have their origin in the water protons, that is, the b population. We therefore assumed the measured  $T_1$  of the IGEL materials to be described in eq 6.

The approach used in fitting the IGEL  $T_1$  data was therefore to employ a method similar to that described previously for the treatment of the  $T_2$  data,<sup>9</sup> with the starting parameters set to those determined in the previous  $T_2$  fits. While the resulting fits were significantly offset from the data, it was found that these fits were also relatively insensitive to the slow motion (bs) correlation time (with activation energy,  $E_{bs}$ , and Arrhenius coefficient,  $\tau_{bs0}$ ) and the weighting factors  $w_{bf}$  and  $w_{bs}$ . These parameters were therefore fixed to the values obtained in fitting the  $T_2$  data. A significant improvement in the fits to the  $T_1$  data could then be achieved by allowing the fast motion (bf) parameters only to vary in the fitting process. The results after this initial round of fitting showed that the resulting values of  $E_{bf}$  and  $\tau_{bf0}$  (bf parameters) were relatively consistent between the three materials.

This sensitivity of the  $T_1$  fits to the bf parameters is expected, since  $T_1$  relaxation is more sensitive to molecular motion with relatively short correlation time (on

**Table 2.**  $T_1$  and  $T_2$  Fit Parameters for the IGEL Materials, Based on Eq 1 (with  $p_c = 0$ ) and Eq 6<sup>a</sup>

hydrogel name	$\tau_{bf0}$ (s)	$E_{bf}$ (kJ/mol)	$\tau_{bs0}$ (s)	$E_{bs}$ (kJ/mol)
IGEL 58	1E-15	28	1.2E-17	54
IGEL 67	3.3E-15	24	2.1E-16	44
IGEL 77	3E-15	23	3.8E-14	31

<sup>a</sup> The accuracy of all fitted parameters lay in the range 5–10%.

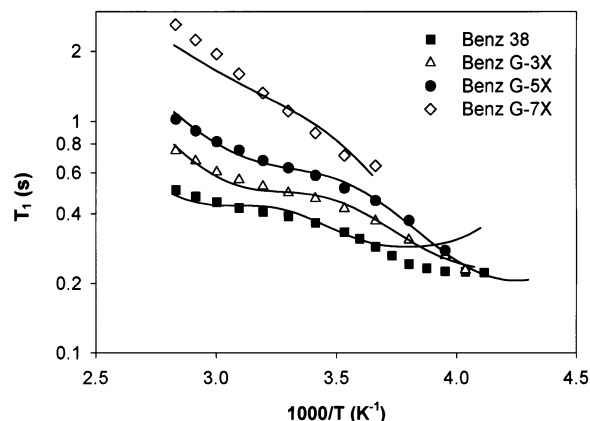


**Figure 3.**  $\ln(T_1)$  as a function of  $1/T$  for the Benz materials. The solid lines are fits to eq 1, using parameters common to the  $T_2$  fits shown in Figure 4.

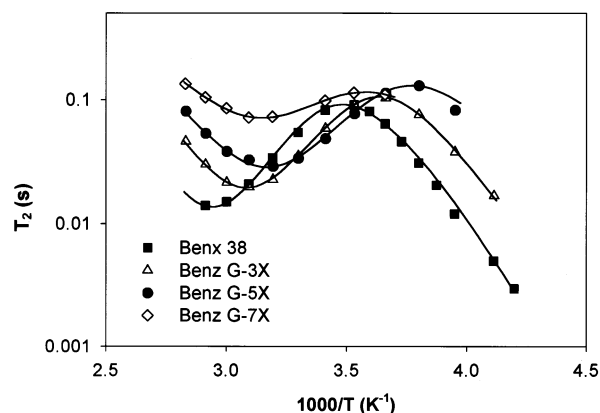


**Figure 4.**  $\ln(T_2)$  as a function of  $1/T$  for the Benz materials. The solid lines are fits to eq 3, using parameters common to the  $T_1$  fits shown in Figure 3.

the order  $\omega_0^{-1}$ ), while as confirmed previously in the  $T_2$  fitting,  $T_2$  relaxation is more sensitive to slower molecular motions. Since the  $T_1$  fits were felt likely to provide a more accurate description of the bf parameters than the  $T_2$  data, the IGEL  $T_2$  data were refitted using these parameters, rather than the previous values which were fixed on the basis of measurements in bulk PBS. In this way, an iterative process was begun, whereby the bs parameters obtained from the new  $T_2$  fits were then used in a new set of  $T_1$  fits, and so on. This process resulted in relatively small changes in the free parameters at each iteration and led to close fits to the data with common parameters for  $T_1$  and  $T_2$  (solid lines in Figures 1 and 2), although there were some small discrepancies—most notably for IGEL 58 at low temperature. The fit parameters are listed in Table 2.

**$T_1$  and  $T_2$  Temperature Dependency and Fitting Considerations—Benz Materials.** Figures 3 and 4 are Arrhenius plots of the temperature dependence of the  $T_1$  and (previously reported<sup>9</sup>)  $T_2$  data for the Benz 38, G-3X, G-5X, and G-7X materials, equilibrated at 80 °C

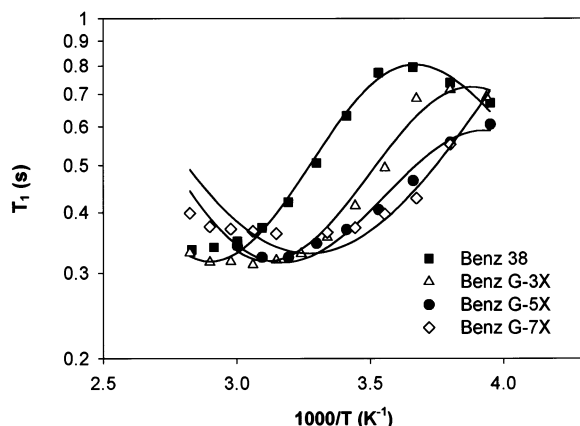


**Figure 5.**  $\ln(T_1)$  as a function of  $1/T$  for the Benz materials hydrated in PBS/D<sub>2</sub>O. The solid lines are fits to the two component exchange model described by eq 7.

in PBS. As in the case of the IGEL materials, both the  $T_1$  and  $T_2$  behavior suggest that multiple correlation times contribute to the observed relaxation. Equation 3 was used to fit the  $T_1$  data, using the values obtained from the previous  $T_2$  fits<sup>9</sup> as starting parameters. However, it became apparent that these fits could not be improved as easily as for the IGEL materials, with the best fits showing significant systematic variation from the data. This highlighted the need to better characterize the  $T_1$  behavior of the polymer protons.

In modeling the  $T_2$  data, the c species was adequately described by a single correlation time, thought to reflect only the motion of the exchangeable protons on the polymer side chains. However, in the case of  $T_1$ , where for reasons explained previously *all* polymer protons contribute to the observed relaxation, a single correlation time is not sufficient to adequately describe all the motional processes of the polymer protons which now need to be considered. Therefore, to directly determine the polymer contribution to the measured spin–lattice relaxation times,  $T_1$  was measured as a function of temperature for samples of the Benz materials that were hydrated in PBS/D<sub>2</sub>O. This effectively removed the signal due to the water protons from the measurements.

**The Polymer Proton Contribution to  $T_1$  for the Benz Materials.** The temperature dependence of  $T_1$  measured for the Benz materials hydrated in PBS/D<sub>2</sub>O is shown in Figure 5. The behavior is complex, with local minima and maxima occurring in some cases. This confirmed that there was more than one distinguishable motion contributing to the polymer  $T_1$  relaxation over the temperature range studied. However, it was found that this behavior could be described reasonably well by the (equally weighted) average of two contributions arbitrarily labeled c1 and c2. Fits were therefore performed using eq 2, where  $T_{1c1}$  and  $T_{1c2}$  are the intrinsic relaxation times of each component, such that

$$\frac{1}{T_{1c}} = \frac{0.5}{T_{1c1}} + \frac{0.5}{T_{1c2}} \quad (7)$$

The fits are shown by the solid lines in Figure 5, with the fitted parameters listed in Table 3. This approximation allowed us to fix the contribution of the polymer protons to  $T_1$  during fitting of the data in which the water protons contribute (Figure 4), ultimately leading to improved results.

**$T_1$  and  $T_2$  Fitting of the Benz Data.** The Benz  $T_1$  data (Figure 3) were refitted with the polymer contribu-

**Table 3.** Fit Parameters for the Benz Materials Hydrated in PBS/D<sub>2</sub>O, Based on Eq 7<sup>a</sup>

hydrogel name	$\tau_{c1,0}$ (s)	$E_{c1}$ (kJ/mol)	$\tau_{c2,0}$ (s)	$E_{c2}$ (kJ/mol)
Benz 38	2.9E-14	28	1.3E-14	19
Benz G-3x	3E-14	26	5.3E-15	20
Benz G-5x	8E-14	23	5.5E-15	20
Benz G-7x	2.8E-13	19	5E-16	19

<sup>a</sup> The accuracy of all fitted parameters is in the range 5–10%.

tion fixed using the parameters listed in Table 3, and this gave significant improvement in the quality of the fitted lines. As for the IGEL materials, it was found that the fits were relatively insensitive to the bs parameters. Also, the weighting factors showed no systematic variation with EWC, with the best fits obtained for values similar to those used previously for the  $T_2$  data. Therefore, using similar methodology to that used in fitting the IGEL data, the bs parameters and weighting factors were fixed in fitting the Benz  $T_1$  data, to refine the bf parameters, which in turn were used to refine the bs parameters through new  $T_2$  fits. This iterative process was repeated until a single set of parameters provided a good description of both the  $T_1$  and  $T_2$  data for the Benz materials. The final best fits are shown by the solid lines in Figures 3 and 4, and the fitted parameters are listed in Table 4. Close fits to the  $T_2$  data were obtained in all cases. For  $T_1$ , however, while the fits to the Benz G-3X and G-5X data were reasonably good, there were clearly some systematic discrepancies in the fits to the Benz 38 and Benz G-7X data.

**Trends in the Fitted Parameters.** To examine trends in both water and polymer mobility, and thereby infer information about water binding, we plotted both the fitted activation energies ( $E_a$ ) and Arrhenius coefficients ( $\tau_{a0}$ ), where  $\alpha$  corresponds to a contributing molecular motion or the chemical exchange process (labeled as “ex”), as functions of measured EWC. The Arrhenius coefficients were plotted on a logarithmic scale. Figures 6 and 7 show these plots for IGEL and Benz water protons, and Figures 8 and 9 show similar plots for the Benz polymer protons, including the hydroxyl proton parameters obtained from the  $T_2$  data. Some clear trends emerge in these data, with the activation energies generally showing a decrease with increasing EWC and the Arrhenius coefficients showing an increase with increasing EWC. Exceptions occur in the case of the bf parameters, which show relatively little change over the range of equilibrium water contents spanned by our samples. The behavior of the Benz G-7X hydrogel appeared anomalous in this respect. For the Benz materials, the polymer proton c2 parameters also seem to show little change with EWC (Figures 8 and 9), again except for Benz G-7X, which has an anomalously low  $\tau_{c2,0}$  value (Figure 9).

While similar values of the bf parameters for both IGEL and Benz materials were found at a given EWC, the IGEL materials exhibit lower  $E_{bs}$  and higher  $\tau_{bs0}$  values than the Benz materials at a given EWC (Figures 6 and 7). However, the *slopes* of these trend plots appear similar between the IGEL and Benz materials, with the curves being approximately parallel. In contrast, the slopes of the exchange parameters,  $E_{ex}$  and  $\tau_{ex0}$ , are significantly lower in these plots.

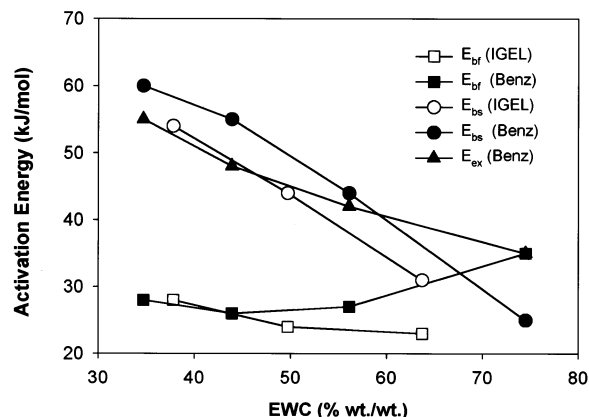
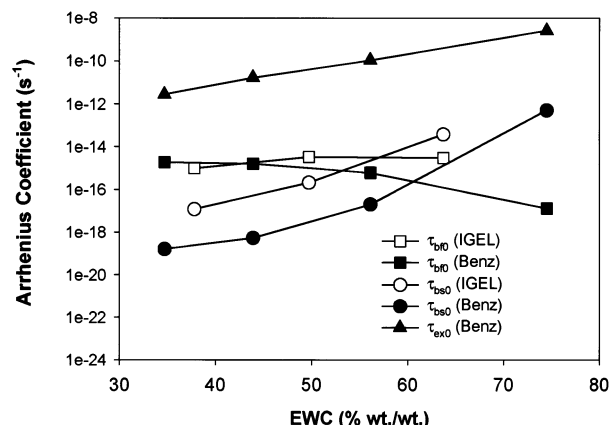
## Discussion

While <sup>1</sup>H NMR has been widely used as a method of studying water mobility and binding in hydrogel

**Table 4.** Fit Parameters for the Benz Materials Based on Eqs 1 and 2<sup>a</sup>

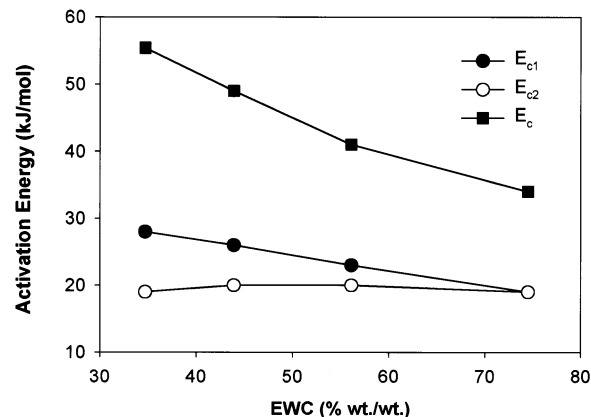
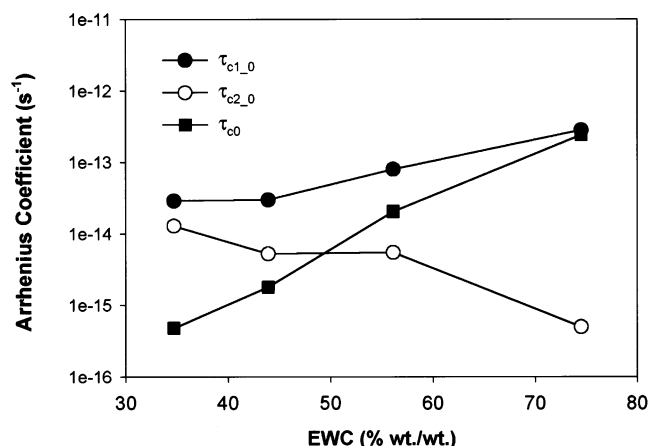
hydrogel name	$\tau_{bf0}$ (s)	$E_{fs}$ (kJ/mol)	$\tau_{bs0}$ (s)	$E_{bs}$ (kJ/mol)	$\tau_{c0}$ (s)	$E_c$ (kJ/mol)	$\tau_{ex0}$ (s)	$E_{ex}$ (kJ/mol)	$p_c$	$P_c$
Benz 38	1.9E-15	28	1.6E-19	60	4.8E-16	55.4	2.8E-12	55	0.115	0.57
Benz G-3x	1.6E-15	26	5.3E-19	55	1.8E-15	49	1.7E-11	48	0.091	0.47
Benz G-5x	6E-16	27	2E-17	44	2.1E-14	41	1.1E-10	42	0.068	0.35
Benz G-7x	1.3E-17	35	5E-13	25	2.4E-13	34	2.6E-09	35	0.036	0.19

<sup>a</sup> Note that the weighting factors  $w_{bf}$  and  $w_{bs}$  were fixed to values of 0.98 and 0.02, respectively.

**Figure 6.** Activation energies derived from the exchange model for  $T_1$  and  $T_2$  relaxation, plotted as a function of measured EWC for the hydrogels studied.**Figure 7.** Arrhenius law coefficients derived from the exchange model for  $T_1$  and  $T_2$  relaxation, plotted (on a log scale) as a function of measured EWC for the hydrogels studied.

polymers,<sup>5-12</sup> the  $T_1$  and  $T_2$  behavior of these materials has proven to be very complex. This is largely due to the effects of magnetization transfer via chemical exchange and spin diffusion which mean that the measured relaxation times may represent the contribution of several different proton "pools", originating from both water and the polymer. The potential for anisotropic molecular motion to occur due to restricted mobility adds further complexity when attempting to quantify water mobility and binding using  $T_1$  and  $T_2$ .

Information about the individual contributions of each contributing proton pool, or strictly speaking, each *molecular motion*, can be obtained by a consideration of the temperature dependency of the measured  $T_1$  or  $T_2$ , assuming a BPP model for relaxation and an Arrhenius activation law for the motional correlation times. The intrinsic  $T_1$  and  $T_2$  values are then obtained via an exchange model that describes magnetization transfer. While we have previously shown excellent agreement of  $T_2$  data with such a model,<sup>9</sup> it was proposed that  $T_1$  would provide a more accurate deter-

**Figure 8.** Activation energies derived from the model for the polymer protons, plotted as a function of measured EWC for the Benz materials. Note that parameters  $E_{c1}$  and  $E_{c2}$  characterize the motion of all the polymer protons, while  $E_c$  refers to the exchangeable (hydroxyl) protons only.**Figure 9.** Arrhenius law coefficients derived from the model for the polymer protons, plotted (on a log scale) as a function of measured EWC for the Benz materials. Note that parameters  $\tau_{c1,0}$  and  $\tau_{c2,0}$  characterize the motion of all the polymer protons, while  $\tau_{c0}$  refers to the exchangeable (hydroxyl) protons only.

mination of the parameters describing the more rapid molecular motion occurring in the water molecules. Therefore, we measured  $T_1$  for some of the same materials that were used in the  $T_2$  measurements and used the same basic exchange model to describe both data sets with common parameters.

A detailed discussion of the origin of the multiple correlation times for the water protons (bs and bf species) has already been provided.<sup>9</sup> Briefly, this behavior is consistent with the presence of two distinct classes of water molecules, with motion on different time scales due to the effects of binding by the polymer, but which are in rapid exchange on the NMR time scale at the temperatures of interest. However, our results do not discount the alternative possibility of a single pool of water having more than one distinct motion (anisot-

ropy). The former is analogous to the concept of relatively "bound" and relatively "free" water and may be more consistent with the findings of previous authors.<sup>10,13</sup> Therefore, in the remainder of the discussion we will refer to separate water proton "species". For the Benz materials, the effect of chemical exchange of water and hydroxyl protons must also be taken into account. The data therefore also provide a description of molecular motion of these hydroxyl protons (the c species for  $T_2$ ) as well as the rate of their chemical exchange with water protons.

**A Single Model for  $T_1$  and  $T_2$  Relaxation.** In the current work, we have shown that the previously proposed model for  $T_2$  can be successfully applied to  $T_1$  data for both Benz and IGEL materials, but with the added provision that for the Benz materials *all* polymer protons contribute through the combination of spin diffusion and chemical exchange. In an iterative process we obtained common fit parameters that generally described close fits to both the  $T_1$  and  $T_2$  data sets (Figures 1–4). This resulted in relatively minor changes to most of the previously fitted parameters (for  $T_2$ ), except the bf parameters, which were significantly refined in the  $T_1$  fitting process and therefore represent more accurate values.

In the previous work, the bf parameters were fixed to values measured in bulk PBS, but in reality it is likely that even the relatively "free" water in a hydrogel is significantly modified in its motion by the polymer, for example in terms of translational mobility. Hence, the bf parameters obtained in the current work are likely to be a truer representation of the relatively "free" water. Therefore, we believe this unified model for  $T_1$  and  $T_2$  provides a more accurate description of the molecular motion and interaction of the individually contributing species.

**Limitations of the Model.** While in general the fitted data were described reasonably closely by the fits to the  $T_1/T_2$  exchange model, there are some systematic discrepancies, most notably for the  $T_1$  fits to the Benz 38, Benz G-7X, and IGEL 58 data.

For Benz 38, while a good description of the  $T_2$  data was obtained, a good fit to the  $T_1$  data could not be obtained, even independently of fitting the  $T_2$  data, particularly at the lower temperatures (Figure 3). While there is no obvious explanation for this, since the Benz 38 material was the lowest EWC material used (34.7%), it is possible that at this water content there is significant deviation from the model for  $T_1$ . We speculate that this could be due to a transition in water binding or water/polymer mobility as temperature decreases. Since this did not affect the  $T_2$  fits, it is suggested that such a transition has affected one or more of the *rapid* molecular motions occurring, since  $T_1$  and not  $T_2$  will be sensitive to this type of motion. This could involve either the bf water component or the c1 or c2 polymer protons, all of which exhibit motion on a time scale comparable to  $\omega_0^{-1}$ .

The fit to the IGEL 58  $T_1$  data also showed discrepancies in the low-temperature region (Figure 1). IGEL 58 is the material with the second lowest EWC (37.8%), and this may again have contributed to anomalous water binding properties at the lower temperatures.

For Benz G-7X, while the  $T_2$  fit was again very good, the best  $T_1$  fit that could be obtained to this model was relatively poor (Figure 3). It is interesting that this material lies at the other extreme of the EWC range of

the materials we studied, having by far the highest value (74.5%). It is again possible that the mobility of one or more of the proton species with rapid motion undergoes a transition at this high EWC, consistent with the systematic deviation of the fitted line from the data over the entire temperature range. The deviation from the model for this material exists at all temperatures studied and may therefore be due to the high EWC alone. Furthermore, freezing of some or all of the water was observed to occur for the Benz G-7X material at the lowest temperatures, resulting in both  $T_1$  and  $T_2$  transitions (data not shown). The Benz G-7X is also a relatively opaque material and has not been approved for use on the eye. These anomalies may cause deviation from the model as evidenced by the discrepancies observed in the  $T_1$  fit.

Other more minor systematic variations in the fits were observed, for both the IGEL and Benz materials. For the IGEL materials, these may have related to the assumption of negligible magnetization transfer between water and polymer protons. While no exchangeable polymer protons exist in these hydrogels, it is still possible for "through-space" cross-relaxation to occur. Small contributions from this process that may have been modulated by temperature may explain some of the minor fit discrepancies, particularly at high temperature in the case of  $T_2$  for IGEL 67 and 77.

While the Benz  $T_2$  fits were generally very good, small variations between the trend of the fitted curves and the data were seen in the case of  $T_1$  for the Benz G-3X and G-5X materials, possibly due to errors in fitting the polymer  $T_1$  data (Figure 5). For the polymer protons, we used a model that is most probably an oversimplification (see below), and since the proportion of polymer protons that contribute in the case of  $T_1$  ( $P$ ) is relatively large (Table 1), this may cause the small systematic inconsistencies observed in the fits. In fact, the poorest of the polymer  $T_1$  fits was observed for Benz G-7X (Figure 5), and this may relate to the relatively large error in the Benz G-7X fit shown in Figure 3.

**$T_1$  Behavior of the Polymer Protons for the Benz Materials.** It is not surprising that more than one correlation time was required to fit the Benz polymer  $T_1$  data (Figure 5), since it is known that relaxation processes in polymers can be related to the onset of motions of various distinct regions of the polymer chain.<sup>16</sup> For example, the side-chain protons may exhibit different motions from backbone or methyl protons.<sup>17</sup> Also, the assumption that the molecular dynamics of a polymer chain can be described by a single correlation time may be simplistic as polymer protons may experience highly anisotropic motions. This motion may depend on multiple internal motions (e.g., rotations associated with conformational changes and torsional motions within a given conformation) as well as overall molecular reorientations arising from cooperative movements of chain segments.

Despite these considerations, we were able to describe  $T_1$  data measured directly from the polymer protons only (in D<sub>2</sub>O/PBS hydrated materials) using a simple two-component correlation time model. In reality, the polymer motional behavior is undoubtedly more complex, and this is evidenced by the imperfect nature of the fits to the data. However, our results show that this model is a good first approximation. As in the case of the water, the separate correlation times for the polymer protons could be due to the distinct motion of different



polymer groups on a relatively rapid time scale or anisotropic motion of the polymer protons as a whole. The polymer side chains are thought to exhibit relatively slow "flip-flop" type motion, which is consistent with the correlation times found for the c species (hydroxyl) protons in our  $T_2$  model ( $\tau_c \sim 10^{-8}$ – $10^{-3}$  s in the temperate range studied). However, likely candidates for the more rapid motions described by the Benz polymer  $T_1$  data ( $\tau_{c1} \sim 10^{-10}$ – $10^{-8}$  s;  $\tau_{c2} \sim 10^{-12}$ – $10^{-10}$  s in the temperate range studied) are more labile species, such as methyl protons, which exhibit rapid reorientational motion. The second component could then be due to rapid reorientation of side chains, for example. However, we have no direct evidence of the origin of these correlation times and cannot discount the possibility of anisotropic motion of the polymer proton pool as a whole.

**Behavior of the Fitted Parameters.** The trends we found for the water proton species with slower motion (bs) indicate an approach toward the values measured for bulk PBS ( $\tau_0 = 5 \times 10^{-13}$  s;  $E_A = 8.6$  kJ/mol ref) with increasing EWC, for both IGEL and Benz materials. This is consistent with less restricted motion being imparted to the water molecules by the polymer as EWC increases. However, the curves for the IGEL materials are offset from those of the Benz materials toward the PBS values and therefore indicate increased mobility or decreased binding in these hydrogels at a given EWC. This is consistent with the relative strengths of the chemical binding groups found in these copolymers. While the Benz materials are expected to obtain their binding characteristics through the very hydrophilic hydroxyl groups, the IGEL materials bind water through relatively weaker hydrogen bonding between water molecules and amide groups. However, the similar slopes of the IGEL and Benz data suggest that a similar relative increase in average water binding results from a given decrease in EWC. The slopes for the  $E_{ex}$  and  $t_{ex}$  are lower and indicate that the chemical exchange between water and polymer protons in the Benz materials, while becoming more rapid with increasing EWC, is less sensitive to a given change in EWC than the specific mobility of the more slowly reorienting (bs) water molecules/motions.

In contrast to the bs behavior, the water species exhibiting relatively rapid motions (bf) shows little change in mobility with EWC, allowing for anomalous values for the Benz G-7X material. These results suggest that the bf component, while being significantly modified with respect to bulk water, is well approximated by motional behavior that is not largely dependent on the EWC. This is consistent with the concept of "bound" and "free" water. In this model, the bs species originates from a small proportion of water (2%) which is associated very closely with polymer binding groups (relatively "bound" water). The remainder of the water is then relatively "free" but has restricted mobility due to the surrounding polymer chains, for example due to a hindrance of translational motion. As the EWC increases, only the proportion of this component increases and not its average mobility.

Figures 8 and 9 show that similar trends are found for the polymer protons, based on a single correlation time (c) for  $T_2$  and two equally weighted correlation times for  $T_1$  (c1 and c2). These trends indicate that plasticization of the polymer by water plays an important role in determining the polymer mobility, contrib-

uting to a synergistic relationship between the water and polymer phases.

The c protons are assumed to originate from exchangeable hydroxyl protons and show similar changes in  $E_c$  and  $\tau_{c0}$  with EWC to that shown by the bs water component. This may reflect the strong interaction between these protons through hydrogen bonding and chemical exchange. The average mobilities of the c1 and c2 components, which represent the entire polymer proton pool, are significantly decreased relative to that of the water molecules and hydroxyl protons, based on their activation energies and Arrhenius coefficients. The parameters of both these components also showed less sensitivity to EWC than the bs and hydroxyl components. These findings are indicative of the decreased mobility expected for large segments of the polymer, when compared to the less restricted motion of water molecules and freely exchanging hydroxyl protons. In comparing the c1 and c2 components, increasing mobility with increasing EWC occurs for c1, whereas little change occurs for c2. Therefore, while the c1 motion may be from more large-scale reorientations of polymer segments which are sensitive to changes in EWC, the c2 motion may be from slower internal motion within these segments which is not largely EWC dependent.

## Conclusions

The results of this study show that a simplified exchange model for the complex  $^1\text{H}$  NMR  $T_1$  and  $T_2$  relaxation in contact lens hydrogels above temperatures at which significant freezing occurs can be applied to a range of materials using a common set of parameters. These parameters describe the contributing molecular motions of both water and the polymer. This both adds validity to this relatively simple model as well as providing a more accurate description of the fitted parameters, which characterize motions on widely varying time scales. In the case of the water molecules, the model is consistent with either two separate classes of water with different average binding properties or a single species showing average anisotropic motion. In the  $T_2$  case, the polymer protons only contribute through exchangeable hydroxyl protons, whereas in the  $T_1$  case, two correlation times were needed for the polymer protons, again suggesting either separate proton groups or all polymer protons being describable in terms of an overall average anisotropic motion.

The fit results suggest that the average mobilities of both water and the polymer are largely dependent on the EWC, although small differences in average binding at a given EWC between the IGEL and Benz hydrogels were found. The results also suggested that the relative increase in binding that occurs with a given decrease in EWC is similar for the IGEL and Benz copolymer formulations. These findings are generally consistent with clinical findings, which suggest that hydrogels with greater EWC dehydrate more on the eye.

Our findings highlight the potential for hydrogels of varying composition and EWC to be characterized in a practical and quantifiable manner, in terms of water binding and mobility, using  $^1\text{H}$  NMR. This methodology may allow new materials with significantly better water binding properties to be identified and could also be used to predict water binding properties for a given copolymer, when formulated to achieve a particular EWC. Although we applied the technique to contact lens polymers, it should be equally applicable to other hydrogel formulations.

## References and Notes

- (1) Peppas, N. A.; Huang, Y.; Torres-Lugo, M.; Ward, J. H.; Zhang, J. *Annu. Rev. Biomed. Eng.* **2000**, *2*, 9–29.
- (2) Kofinas, P.; Cohen, R. E. *Biomaterials* **1997**, *18*, 1361–1369.
- (3) McConville, P.; Pope, J. M. *CLAO J.* **2001**, *27*, 186–191.
- (4) Roorda, W. *J. Biomater. Sci., Polym. Ed.* **1994**, *5*, 383–395.
- (5) Roorda, W.; de Bleyser, J.; Juginger, H. E.; Leyte, J. C. *Biomaterials* **1990**, *11*, 17–23.
- (6) Mathur, A. M.; Scranton, A. B. *Biomaterials* **1996**, *17*, 547–557.
- (7) Manetti, C.; Casciani, L.; Pescosolido, N. *Polymer* **2002**, *43*, 87–92.
- (8) Larsen, D. W.; Huff, J. W.; Holden, B. A. *Curr. Eye Res.* **1990**, *9*, 697–706.
- (9) McConville, P.; Pope, J. M. *Polymer* **2001**, *42*, 3559–3568.
- (10) Barbieri, R.; Quaglia, M.; Delfini, M.; Brosio, E. *Polymer* **1998**, *39*, 1059–1066.
- (11) McConville, P.; Pope, J. M. *Polymer* **2000**, *41*, 9081–9088.
- (12) McBrierty, V. J.; Martin, S. J.; Karasz, F. E. *J. Mol. Liq.* **1999**, *80*, 179–205.
- (13) Ablett, S.; Lillford, P. J.; Baghdadi, S. M. A.; Derbyshire, W. *J. Colloid Interface Sci.* **1978**, *67*, 355–377.
- (14) Hazelwood, C. F.; Chang, D. C.; Nichols, B. L.; Woessner, D. E. *Biophys. J.* **1974**, *14*, 583.
- (15) Abragam, A. *The Principles of Nuclear Magnetism*; Clarendon Press: Oxford, 1983.
- (16) Donth, E. J. *Relaxation and Thermodynamics in Polymers: Glass Transition*; Akademik Verlag GmbH: Berlin, 1992.
- (17) Kolarik, J. *Advances in Polymer Science* **46**. Springer-Verlag: Berlin, 1992.
- (18) Benz, P. H.; Orrs, J. A. Contact lens having improved dimensional stability. Benz Research and Development Corp., Sarasota, FL, Patent #5532289.
- (19) Patel, P. G.; Da Costa, N. M. Cross-linked hydrophilic polymers. United States Patent #4361689.

MA020539C